Botanica Pacifica. A journal of plant science and conservation. 2026. 15(1): 3–21
DOI: 10.17581/bp.2026.15108

RESEARCH PAPER

A homogeneous green belt: zonal vegetation of East Asia in the Eocene

Olesya V. Bondarenko[1]* & Torsten Utescher[2,3]

Olesya V. Bondarenko [1]*
e-mail: laricioxylon@gmail.com

Torsten Utescher [2,3]
e-mail: torsten.utescher@senckenberg.de

[1] Federal Scientific Center of the East Asia Terrestrial Biodiversity FEB RAS, Vladivostok, Russia

[2] Senckenberg Research Institute and Natural Museum, Senckenberg Research Station of Quaternary Palaeontology, Weimar, Germany

[3] Steinmann Institute, University of Bonn, Bonn, Germany

* corresponding author

Manuscript received: 23.01.2026
Review completed: 21.02.2026
Accepted for publication: 23.02.2026
Published online: 24.02.2026

Electronic Appendix

(1) http://www.geobotanica.ru/bp/2026_15_01/BP_2026_15_1_bondarenko_e_suppl.xlsx

ABSTRACT

Based on a comprehensive analysis of 240 micro- and macrofloras, the reconstruction of zonal vegetation across the paleocontinent Asia for the early, middle, and late Eocene has been performed, refining the model of a homogeneous "green belt." This belt was dominated by Mixed Mesophytic Forests (MMF), a unique biome without modern analogues, characterized by a balanced composition of broad-leaved deciduous (44.3–77.6 %) and evergreen (14.9–29.9 %) taxa. This biome extended into high Arctic latitudes (>75°N), indicating an exceptionally weak meridional temperature gradient during the early Paleogene. Clear latitudinal differentiation was observed: the proportion of evergreen elements increased southward, forming an MMF / Broad-Leaved Evergreen Forest (BLEF) ecotone and pure BLEF south of ~50°N. In central continental regions, a low content of sclerophytic components was noted, suggesting that lithological data on aridity reflect a mosaic of seasonally dry forests and open patches rather than a continuous zonal desert. From the early to late Eocene, a significant trend towards ecological differentiation and provincialization emerged, marked by the appearance of sub-humid sclerophytic forests and open woodlands, correlating with cooling following the Early Eocene Climatic Optimum and increased seasonality. Systematic discrepancies between micro- and macroflora-based reconstructions were identified, attributed to taphonomic and ecological filters, highlighting the complementary nature of these proxies.

Keywords: Eocene, palaeovegetation, Asia, biome reconstruction, Integrated Plant Record, mixed mesophytic forest, climate gradient, aridization

РЕЗЮМЕ

Бондаренко О.В., Утешер Т. Зональная растительность палеоконтинента Азия в эоцене. На основе комплексного анализа 240 микро- и макрофлор выполнена реконструкция зональной растительности палеоконтинента Азия для раннего, среднего и позднего эоцена и уточнена модель гомогенного «зелёного пояса», в котором доминировали смешанные мезофитные леса (MMF), представлявшие уникальный, не имеющий современных аналогов биом, для которого характерен сбалансированный состав широколиственных листопадных (44,3–77,6%) и вечнозелёных (14,9–29,9%) таксонов. Этот биом простирался до высоких арктических широт (>75° с.ш.), что указывает на исключительно слабый меридиональный температурный градиент в раннем палеогене. Наблюдалась чёткая широтная дифференциация: доля вечнозелёных элементов увеличивалась к югу, формируя экотон MMF / широколиственных вечнозелёных лесов (BLEF) и чистые BLEF к югу от ~50° с.ш. В центральных континентальных регионах отмечено низкое содержание склерофитных компонентов, что позволяет предполагать, что литологические данные об аридности отражают мозаику сезонно-сухих лесов и открытых участков, а не сплошную зональную пустыню. С раннего по поздний эоцен наметилась значительная тенденция к экологической дифференциации и провинциализации, выраженная в появлении субгумидных склерофитных лесов и открытых редколесий, что коррелирует с похолоданием после раннеэоценового климатического оптимума и усилением сезонности. Выявлены систематические расхождения между реконструкциями на основе микро- и макрофлор, объясняемые тафономическими и экологическими фильтрами, что подчёркивает комплементарный характер этих прокси.

Ключевые слова: Эоцен, палеорастительность, Азия, реконструкция биомов, комплексный анализ растительного покрова, смешанный мезофитный лес, климатический градиент, аридизация

Vegetation constitutes a fundamental component of terrestrial ecosystems, serving as a primary recorder and integrator of prevailing environmental and climatic conditions. The modern vegetation of Asia is characterized by exceptional heterogeneity, a direct consequence of the continent's vast latitudinal extent, extreme topographic contrasts, and complex climatic regimes – ranging from arctic tundra in the north to perhumid tropical rainforests in the southeast (Krestov 2006). East Asia, in particular, hosts the world's most extensive meridional forest gradient, spanning over

60° of latitude along the western Pacific margin. This gradient encompasses a vast array of biomes, from boreal taiga to subtropical broadleaved evergreen forests, shaped by a monsoonal climate system and a dynamic geological history. Understanding the long-term evolution of this complex vegetation cover, especially during past periods of global warmings, provides critical insights into the response mechanisms of terrestrial ecosystems to climate forcing, biodiversity dynamics, and the resilience of plant communities under changing boundary conditions (Utescher et al. 2017, Lunt et al. 2021). Such knowledge is indispensable for refining climate-vegetation models used to project future ecosystem changes.

The early Paleogene, and specifically the Eocene epoch (~56 to 34 Ma), represents the most recent sustained phase of global greenhouse conditions in Earth's history, following the thermal maximum of the Paleocene–Eocene boundary and culminating in the descent towards the icehouse world of the Oligocene (Zachos et al. 2008, Westerhold et al. 2020). Characterized by elevated atmospheric CO_2 concentrations and reduced latitudinal temperature gradients, this period saw frost-free conditions extending into high polar regions, which supported extensive forests where today only tundra exists (Willis & McElwain 2002). The globally warm and humid climate facilitated the expansion of diverse thermophilic and mesophilic vegetation, including paratropical rainforests, subtropical broadleaved evergreen forests, and warm-temperate deciduous forests, with biomes occupying significantly higher palaeolatitudes than their modern analogues (Greenwood & Wing 1995, Collinson 2000). Concurrently, the Eocene witnessed a major phase of angiosperm diversification and ecological dominance, with the establishment and radiation of numerous modern families and genera (Wing & Boucher 1998). Consequently, the Eocene greenhouse world offers a crucial deep-time analogue – "natural experiment" – for studying terrestrial ecosystem structure, composition, and biogeography under a climate state potentially analogous to future warming scenarios (Salzmann et al. 2009, Pound et al. 2012, Burke et al. 2018).

Despite its recognized importance, a comprehensive and quantitative understanding of Eocene vegetation patterns across the vast and topographically complex Asian palaeocontinent remains elusive. Early pioneering reconstructions, often based on qualitative comparisons of selected taxa or limited regional datasets, proposed broad-scale models such as a simple latitudinal zonation with a vast interior arid belt (Wolfe 1985) or the existence of a "boreotropical" flora with high-latitude tropical elements (Wolfe 1979). However, these models have been debated and refined as new data emerged, revealing a more complex picture with evidence for significant spatial heterogeneity and the potential influence of proto-monsoonal circulations (Collinson & Hooker 2003, Akhmetiev 2004). Recent advancements have employed quantitative methodologies like the Plant Functional Type (PFT) analysis and the Integrated Plant Record (IPR) vegetation analysis, leading to more robust, data-driven regional reconstructions (e.g., Utescher & Mosbrugger 2007, Kovar-Eder & Teodoridis 2018, Teodoridis et al. 2021, Li et al. 2022, Bondarenko & Utescher 2024b, 2025, Thompson et al. 2025). These studies highlight, for instance, the presence of humid subtropical forests in Central Asia during the early Eocene, challenging the notion of pervasive aridity (Zhang et al. 2012, Bosboom et al. 2014). Nonetheless, significant spatial and temporal gaps persist. Large regions, particularly in Eastern Siberia and the Russian Far East (RFE), remain underrepresented in continental-scale syntheses (Herman et al. 2017). This fragmented picture hinders the resolution of key debates regarding the dominant climatic controls – whether a static zonal pattern prevailed or a more dynamic system with significant monsoon-driven precipitation heterogeneity existed (Licht et al. 2014, Bondarenko 2025) – and limits our ability to fully assess biome sensitivity to Eocene climatic fluctuations.

This study aims to address this critical knowledge gap. We present the first comprehensive, quantitative, and spatially exhaustive reconstruction of zonal vegetation for the entire Asian palaeocontinent throughout the successive stages of the Eocene epoch (early, middle, and late). Our analysis is based on a large, meticulously curated palaeobotanical dataset comprising 240 well-dated micro- and macrofloras from 157 localities. By applying the standardized IPR vegetation analysis (Kovar-Eder et al. 2008, Teodoridis et al. 2021), a method designed to translate fossil plant assemblages into defined zonal vegetation types, we transcend purely floristic lists to infer ecosystem structure. The central research question guiding this work is: How did the composition, spatial distribution, and latitudinal boundaries of major zonal vegetation types across Asia change throughout the Eocene in response to evolving global climate, regional palaeogeographic and tectonic conditions?

We hypothesize that Eocene vegetation exhibited a more homogeneous and latitudinally compressed zonal structure compared to the highly fragmented modern Asian vegetation, with thermophilic forest biomes extending to unusually high latitudes. Furthermore, we anticipate detectable biome shifts occurred across the epoch, manifesting as a general southward retreat of warmth-loving vegetation and an expansion of more temperate biomes in response to post-EECO global cooling and increasing continentality in Central Asia. By generating this continental-scale synthesis, this work seeks to provide definitive vegetation-based evidence to clarify Asia's Eocene climatic setting and establish a robust benchmark for understanding terrestrial ecosystem dynamics under prolonged greenhouse conditions.

MATERIAL AND METHODS

Study area and stratigraphic framework

The palaeobotanical records analyzed herein originate from 157 localities across Asia (Fig. 1; Supplementary electronic information 1). The Eocene deposits of the study region are widespread and predominantly terrestrial.

In China, Eocene strata are widely distributed, with facies ranging from fluvial-lacustrine in the east to evaporitic redbeds in the interior (Li 1984). While the age of many floras was historically assigned broadly (e.g., epoch-level), recent interdisciplinary studies integrating magnetostratigraphy, radiometric dating, and biostratigraphy have significantly improved chronological constraints (e.g., Huang et al. 1998,

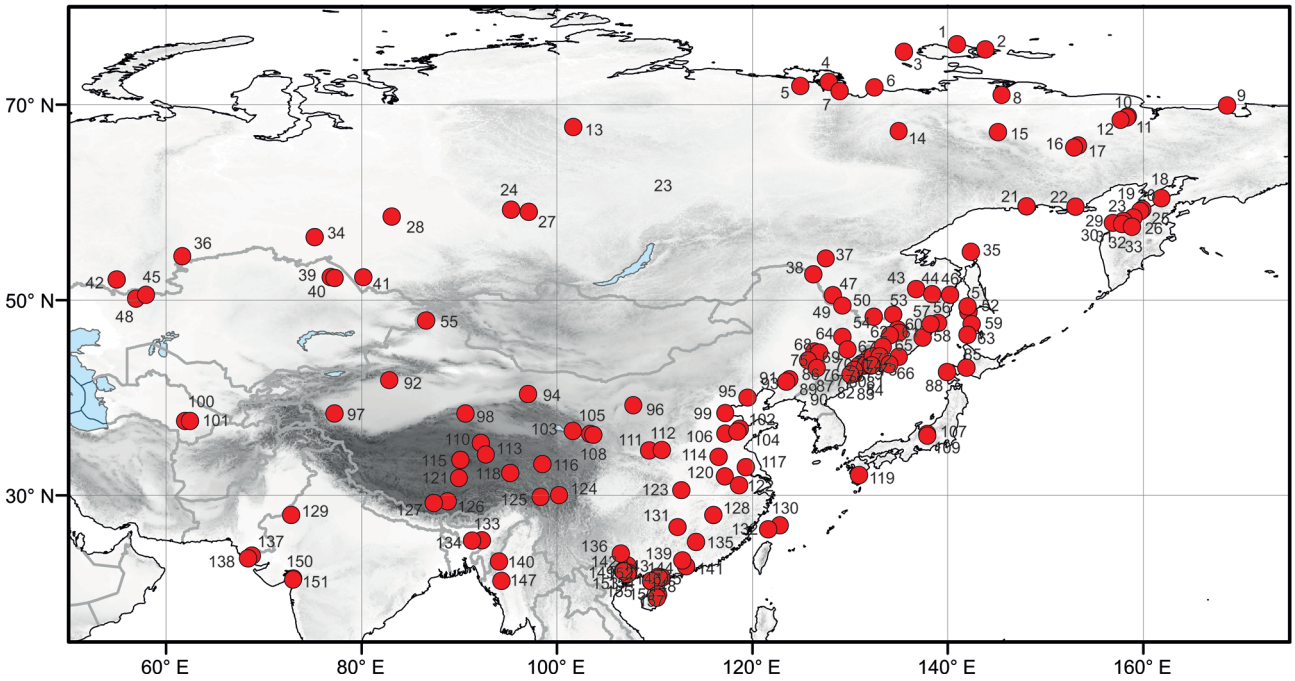

Figure 1 Geographical distribution of flora study sites during the Eocene. The localities are listed in Supplementary electronic information 1

Wang et al. 1999, Miao et al. 2008, Shi et al. 2008, Pei et al. 2009), enabling stage-level reconstructions (Quan et al. 2012).

The regions of RFE and Eastern Siberia are characterized by extensive non-marine deposits. In the southern RFE, volcanic-sedimentary successions with intercalated lignites fill basins affected by rifting and regional tectonics (Pavlyutkin & Petrenko 2010). Northern and eastern sections (e.g., Kamchatka, Sakhalin, the Anadyr Basin, and coastal basins of the Siberian Platform) contain isolated Cenozoic deposits overlying folded Mesozoic basement.

The area of Western Siberia (Tobol/Ob River Basins) was part of the Turgai Strait, connecting Arctic and Para-Tethyan seas during the Late Cretaceous–Paleogene (Vasilieva & Levina 2007). Paleogene deposits (~400 m thick) are widespread, with marine facies dominating the section; continental facies are typically restricted to the uppermost part. Biostratigraphy relies heavily on dinoflagellate cysts due to the scarcity of calcareous microfossils (Amon 2001, 2018).

Regional stratigraphic correlations (Supplementary electronic information 2) follow established schemes: Quan et al. (2012) for China; Kezina (2005) and Pavlyutkin & Petrenko (2010) for the continental southern RFE; Gladenkov et al. (2002) for Sakhalin; Gladenkov et al. (2005) for Kamchatka; and Grinenko et al. (1997) for northern RFE and Siberia. Age control for the selected floras is based on multi-proxy data, including radiometric, palaeomagnetic, and biostratigraphic (palynological, macrofloral, faunal) evidence, tied to the International Chronostratigraphic Chart (Cohen et al. 2013, updated). This allows assignment of flora-bearing horizons to the stage level, with higher resolution for some key sites (Supplementary electronic information 1 & 2).

Floral record

We analyzed a total of 240 palaeofloras from Western/Eastern Siberia, the RFE, Korea, Kazakhstan, China, India, and Japan, covering the early to late Eocene (~55.8–33.9 Ma). The dataset includes: 174 palynofloras (PF), 64 leaf floras (LF), 1 carpoflora (CF) and 1 xyloflora (XF).

The floras were assigned to three time slices – early (Ypresian), middle (Lutetian–Bartonian), and late (Priabonian) Eocene – based on compiled stratigraphic data (Supplementary electronic information 1). Fourteen sites (e.g., Alchan, Bikin, Fushun) provide multiple floristic levels spanning the entire epoch, ensuring temporal consistency. Twenty-nine levels contain both micro- and macrofloral records.

For the early Eocene, a total of 83 floras (67 PF, 16 LF) is available, all within the range from 21.25 to 76.06°N and from 61.71 to 145.60°E. For the middle Eocene, the compilation comprises 84 floras (57 PF, 25 LF, 1 CF and 1 XF) within the range from 19.38 to 75.53°N and from 58.00 to 168.66°E. The late Eocene record includes 73 floras (50 PF, 23 LF) covering the range from 20.60 to 71.70°N and from 57.00 to 161.96°E.

All taxonomic identifications and assignments of Nearest Living Relatives (NLRs) were critically re-evaluated. Complete flora lists, NLR assignments, and references are provided in Supplementary electronic information 2.

Assigning to IPR components

Vegetation reconstruction employed the IPR analysis, a semi-quantitative method designed to assess zonal vegetation from fossil plant assemblages (Kovar-Eder & Kvaček 2003, Teodoridis et al. 2021). The method involves assigning all taxa from an assemblage to one of thirteen taxonomic-physiognomic components based on their NLR ecology:

I. Zonal components:
1. CONIF: Conifers
2. BLD: Broadleaved deciduous angiosperms
3. BLE: Broadleaved evergreen angiosperms
4. SCL: Sclerophyllous angiosperms
5. LEG: Legume-like taxa (often merged with SCL)
6. ZONPALM: Zonal palms
7. ARBFERN: Arborescent ferns

8. D-HERB: Dry herbaceous (e.g., xeric grasses)
9. M-HERB: Mesophytic herbaceous

II. Azonal components:
10. AZW: Azonal woody (riparian, swamp)
11. AZNW: Azonal non-woody
12. AQUA: Aquatic plants
13. PROBLEMATIC: Taxa with uncertain affinity

Taxon allocation to components is detailed in Supplementary electronic information 2. For analysis, the relative proportion of each component within an assemblage is calculated. A minimum of ten zonal taxa per flora is recommended for reliable application (Kovar-Eder et al. 2008). Later, Kovar-Eder & Teodoridis (2018) raised the former threshold to 15 zonal taxa to apply the IPR-vegetation analysis.

Data processing and vegetation classification (plant biomes)

A cluster analysis (single linkage, squared Euclidean distance) was performed on the matrix of zonal component proportions to group floristically similar sites, using the PAST 4.03 software package (Hammer et al. 2001). Traditionally, cluster analysis is not used when applying the method. However, we think it helps to further decipher larger groups of sites allocated by the IPR threshold procedure, e.g. the large MMF group.

To classify zonal vegetation, we calculated the key component proportions (Supplementary electronic information 3):

1) proportions of woody deciduous angiosperm group, e.g., BLDprop = BLD / (BLD+BLE+SCL+LEG+ZONPALM+ARBFERN);

2) proportions of woody evergreen angiosperm group, e.g., BLEprop = BLD / (BLD+BLE+SCL+LEG+ZONPALM+ARBFERN);

3) proportions of woody SCL+LEG group, e.g., SCL+LEGprop = (SCL+LEG) / (BLD+BLE+SCL+LEG+ZONPALM+ARBFERN);

4) proportion of zonal herbs, e.g., ZONALHERBprop = (D-HERB+M-HERB) / (CONIF+BLD+BLE+SCL+LEG+ZONPALM+ARBFERN+D-HERB+M-HERB);

5) additionally, calculated the proportion of conifers following Bondarenko et al. (2024a), e.g., CONIFprop = CONIF / (CONIF+BLD+BLE+SCL+LEG+ZONPALM+ARBFERN).

Based on established thresholds (Kovar-Eder et al. 2008, Teodoridis et al. 2011), assemblages were classified into six zonal vegetation types:

1. Broadleaved Deciduous Forest (BLDF)
2. Mixed Mesophytic Forest (MMF)
3. Broadleaved Evergreen Forest (BLEF)
4. Subhumid Sclerophyllous Forest (ShSF)
5. Xeric Open Woodland (OWl)
6. Xeric Grasslands or Steppe (Gl/St)

and three their ecotones BLDF/MMF, BLEF/MMF, MMF/ShSF.

Visualization

The geographical distribution of the 157 studied Eocene flora sites across the Asian palaeocontinent is visualized on a base map (Fig. 1). Temporal dynamics in the proportion of conifers (Fig. 2), broadleaved deciduous (Fig. 3), and evergreen (Fig. 4) taxa relative to other plant groups across the Eocene time slices are presented as composite bar charts. Similarly, the temporal dynamics of woody versus herbaceous plant groups are shown in a composite bar chart (Fig. 5). To assess compositional similarity, a cluster analysis (dendrogram) was performed on all studied Eocene floras, grouping them into distinct units (Fig. 6). The distribution of these units is mapped to identify regional patterns and their evolution throughout the Eocene (Fig. 7). Finally, the spatial distribution of the reconstructed IPR-derived major plant biomes for the three Eocene time slices is visualized on base maps (Fig. 8). All maps were prepared using ArcMAP 10.4.

RESULTS

Applicability and reliability of the IPR analysis

A total of 240 floras were analyzed subjected to the IPR vegetation analysis. From these, 29 localities combined micro- and macrofloral data, yielding 211 discrete floral assemblages assigned to zonal vegetation types. The number of fossil taxa per site ranged from 6 to 171, reflecting high variability in preservation and sampling effort.

Applying a reliability threshold of ≥10 zonal taxa per flora, the majority of floras provided robust data. Only 12 floras (5.0 %) across the entire Eocene (3 early, 4 middle, 5 late Eocene) fell below this threshold. A more stringent threshold of ≥15 zonal taxa excluded 34 floras, indicating that a subset of assemblages had limited taxonomic representation. For the remaining floras meeting the ≥10 taxa criterion, the mean number of zonal taxa was 34.46 (std. dev. 16.57), confirming the overall robustness of the dataset for vegetation reconstruction.

Variability of zonal components

The proportional representation of IPR zonal components exhibited high spatial and temporal heterogeneity (Fig. 2–5). BLD showed the greatest range (0–80.5 %) and were the dominant group across most floras. BLE ranged from 0 to 29.1 %, with higher values concentrated in low-latitude sites. CONIF were represented by 0 to 23.5 % and showed a clear latitudinal increase. SCL+LEG were consistently rare (<5 %) except in a few late Eocene sites. ZONPALM (0.5–9.5 taxa) and ARBFERN (1–4 taxa) were present in 72 and 61 floras, respectively, primarily in early Eocene low-latitude records. Herbaceous components (D-HERB, M-HERB) reached up to 24.8% in certain late Eocene floras, signaling the expansion of open habitats. Thus, the dominant plant groups are: CONIF, BLD and BLE. Conifers are significant, especially in certain floras and clusters. Broadleaved deciduous and evergreen taxa dominate many floras. Herbs, palms, and ferns are present but generally subordinate to woody plants.

Cluster analysis of floras

Cluster analysis performed on the matrix of six main zonal component proportions revealed a coherent structure

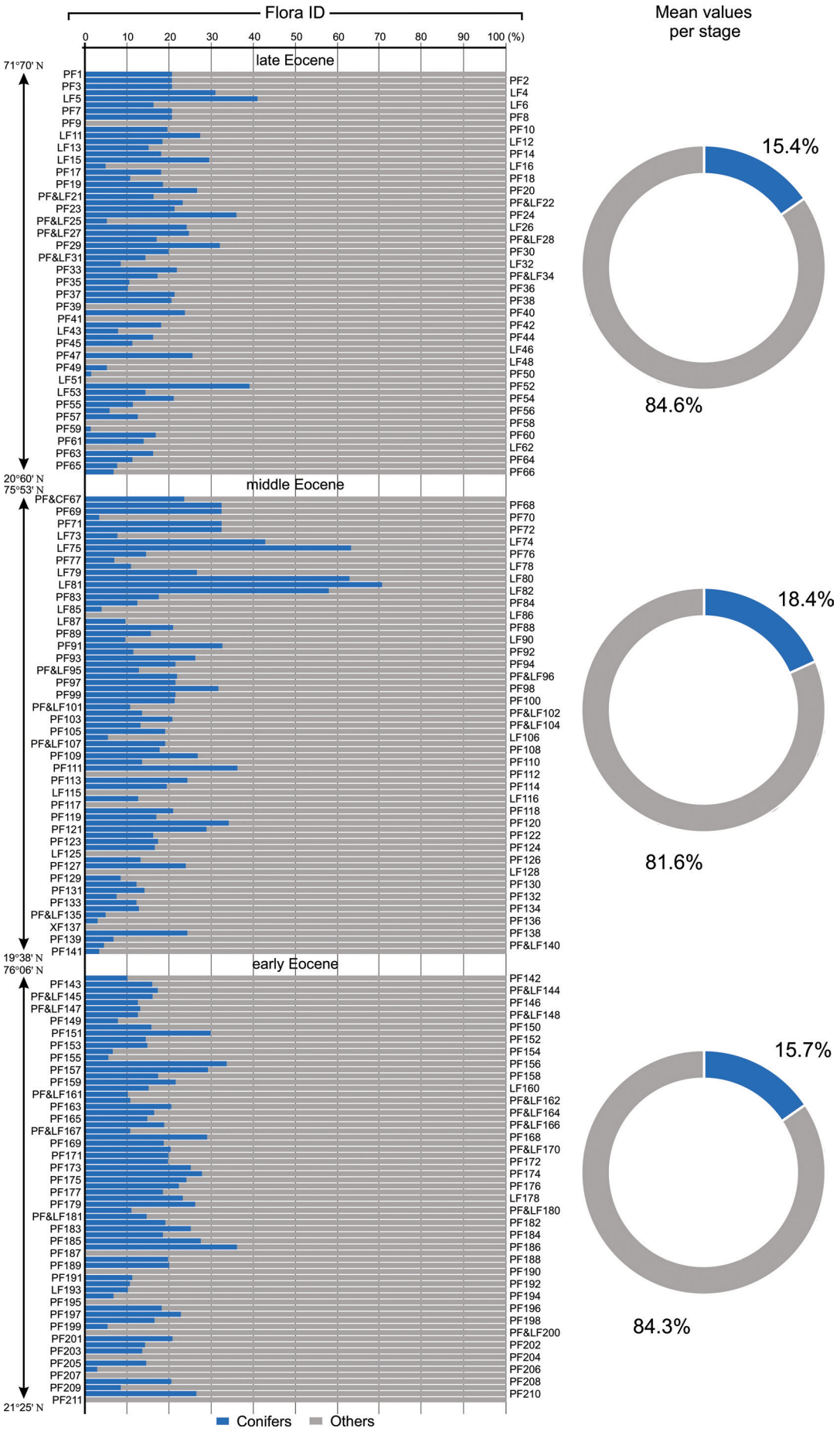

Figure 2 Dynamics of the proportion of conifers (CONIF) and other plant groups in the Eocene floras

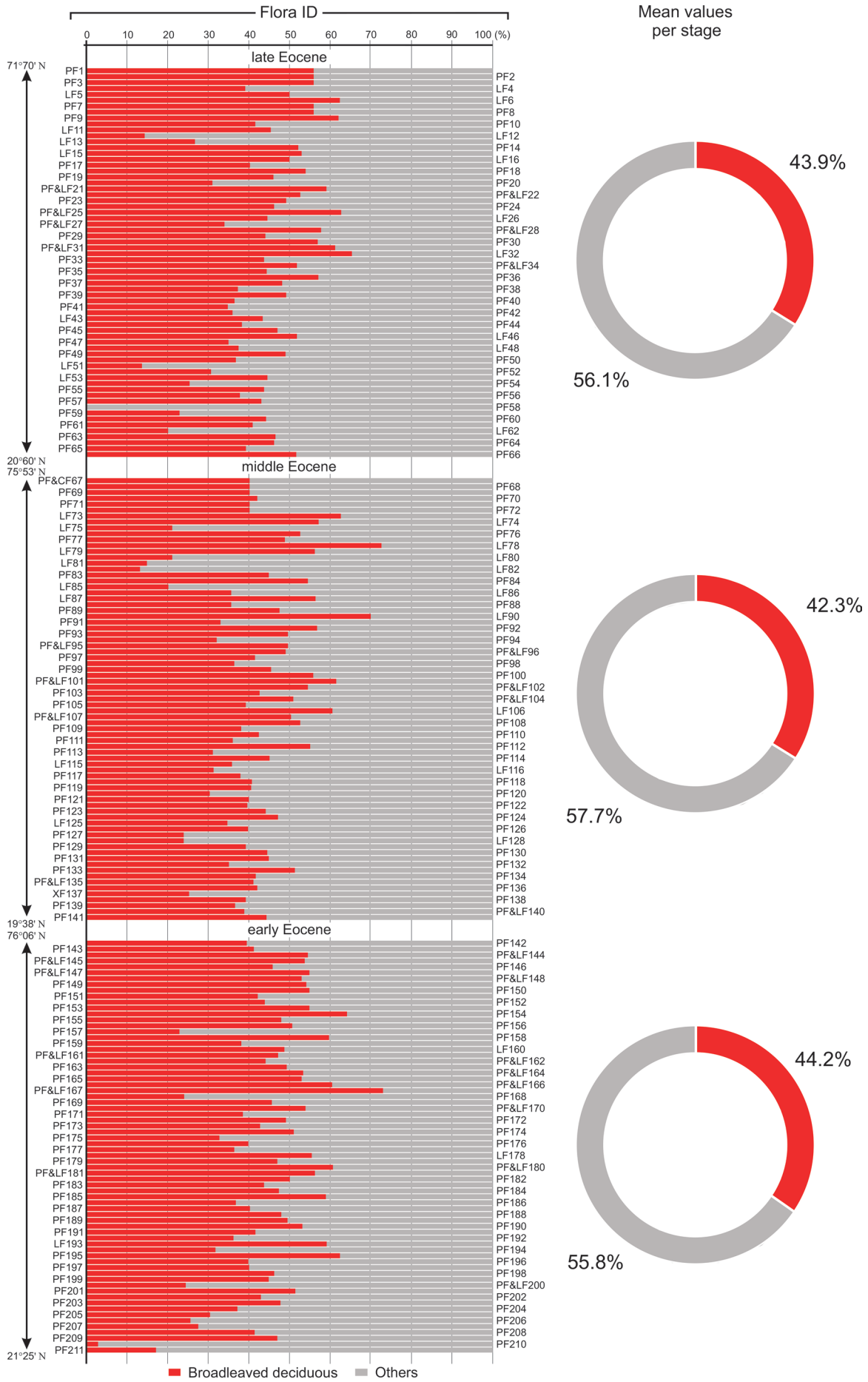

Figure 3 Dynamics of the proportion of broadleaved deciduous (BLD) and other plant groups in the Eocene floras

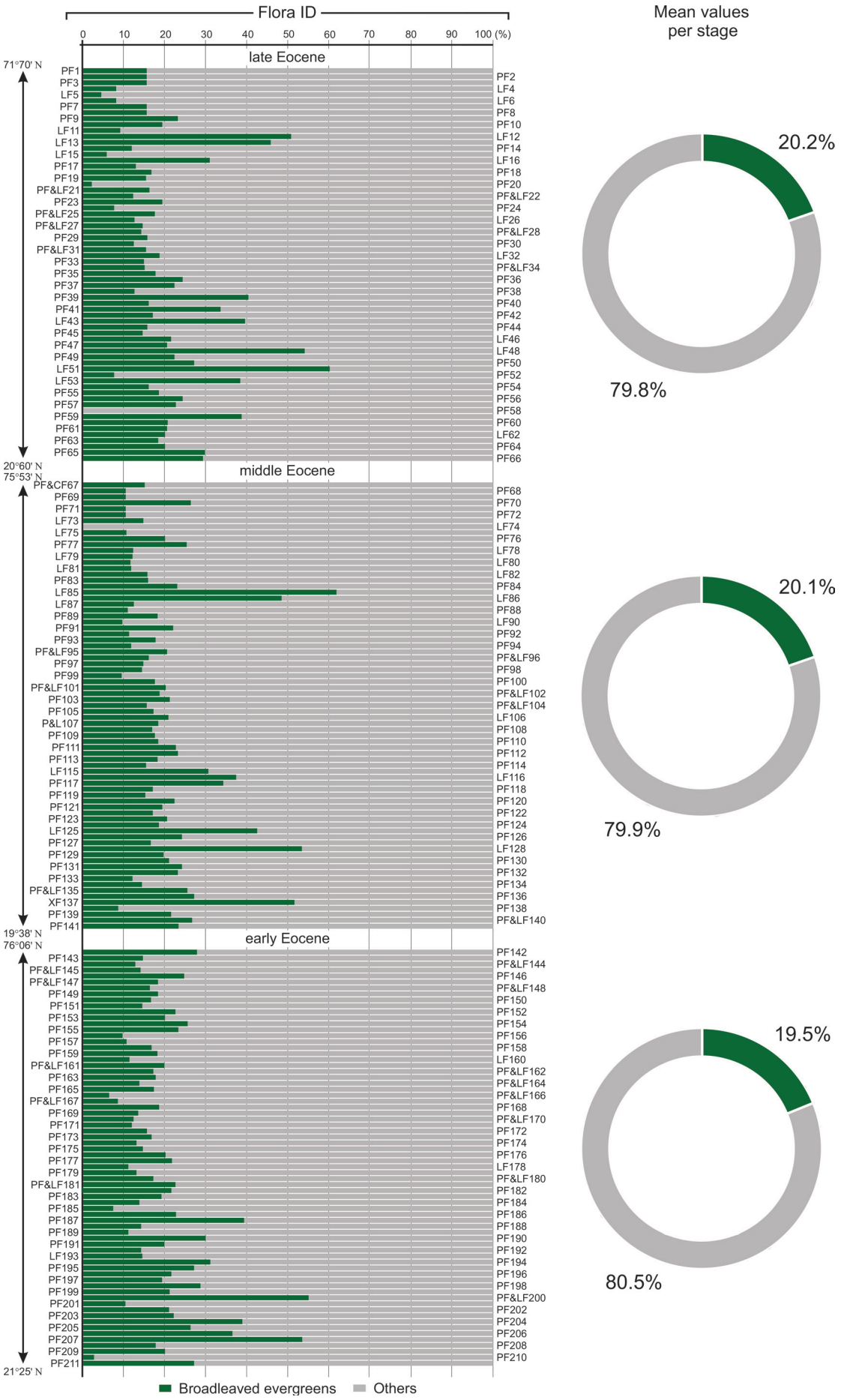

Figure 4 Dynamics of the proportion of broadleaved evergreens (BLE) and other plant groups in the Eocene floras

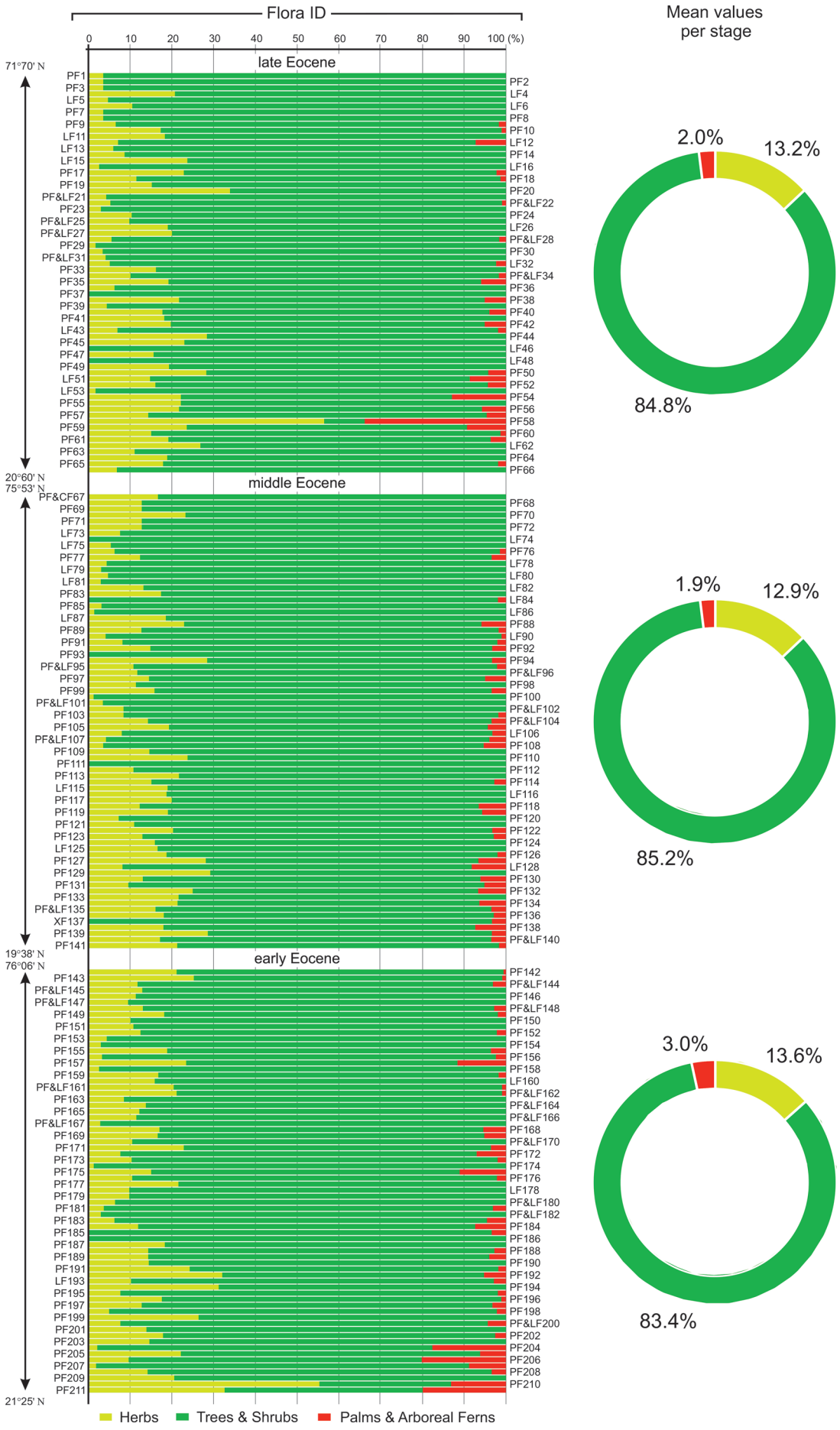

Figure 5 Dynamics of the proportion of woody vs. herbaceous plant groups in the Eocene floras

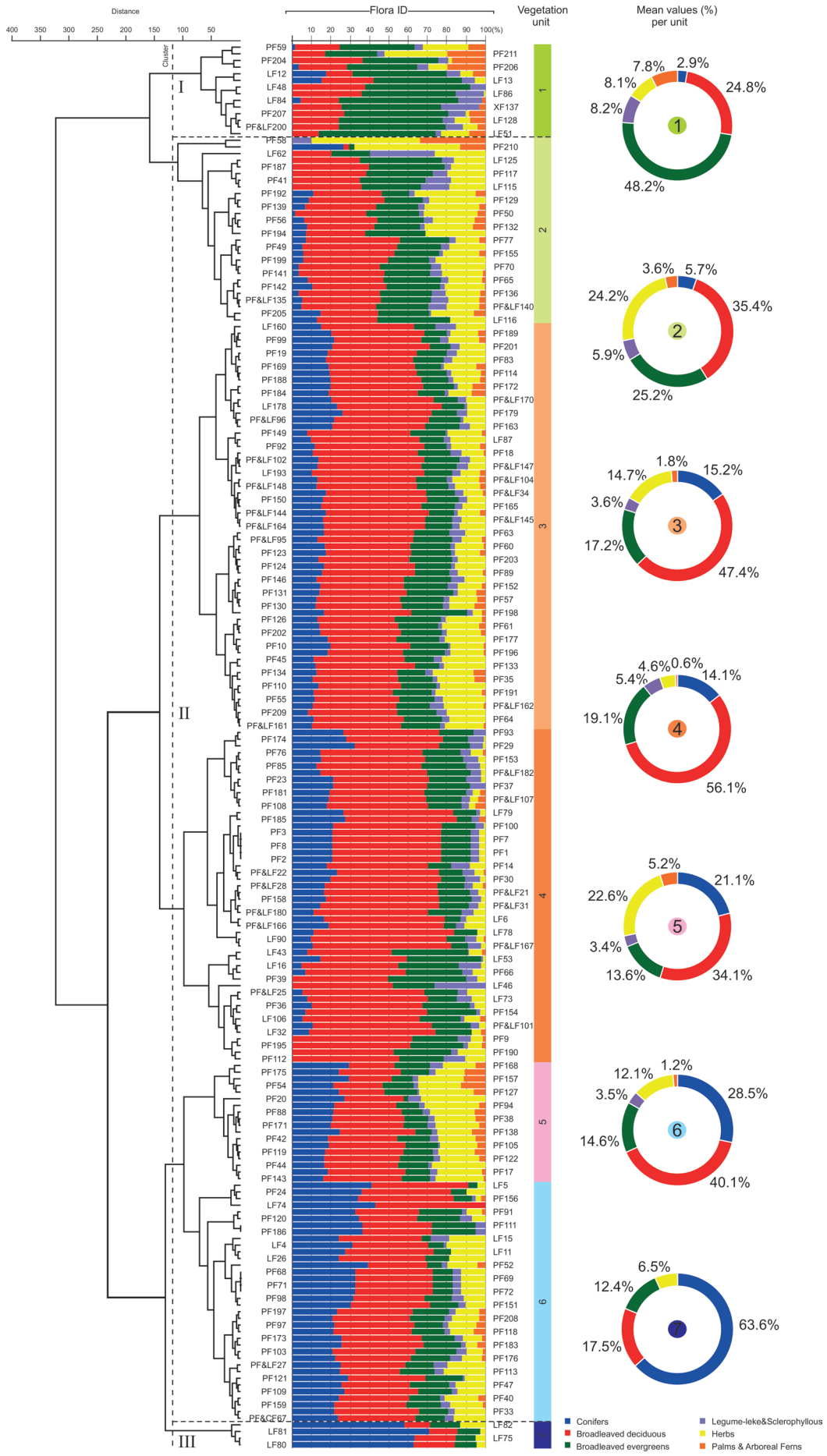

Figure 6 Cluster analysis of Eocene floras

within the dataset (Fig. 6). Seven distinct groups (Vegetation units 1–7) were identified, which can be broadly categorized into three major clusters (I–III):

Cluster I (Unit 1): characterized by the unequivocal dominance of BLE taxa (mean 48.2 %), corresponding to tropical/subtropical BLEFs. This group includes primarily low-latitude floras and exhibits the lowest proportion of conifers (2.9 %).

Cluster II (Units 2–6): dominated by BLD taxa, representing the ecological spectrum of MMFs and, to a lesser extent, BLDFs. These groups are differentiated by their secondary components:

Units 2 & 3: characterized by a significant admixture of BLE taxa (25.2 % and 17.2 %, respectively), representing the core MMF biome with a stronger evergreen influence, typical for mid-latitudes.

Unit 4: distinguished by an exceptionally high proportion of BLD (56.1 %) coupled with very low BLE (5.4 %), likely reflecting the most deciduous-rich variant of MMF or transitional BLDF/MMF communities, often found at higher latitudes or in continental interiors.

Unit 5: marked by a notable increase in herbaceous components (22.6 %), indicating more open forest structures (e.g., woodland) within the MMF framework.

Unit 6: defined by the highest conifer proportion (28.5 %) among Cluster II, representing MMF with a significant coniferous understory or admixture, prevalent in northern and northeastern regions.

Cluster III (Unit 7): defined by the absolute dominance of CONIF (63.6 %), reflecting warm-temperate coniferous-dominated forests. This small group is geographically restricted to a few high-latitude sites.

The spatial distribution of these seven vegetation units across the three Eocene time slices is mapped in Fig. 7. This visualization clarifies the regional preferences and temporal evolution of the floristic subtypes identified by the cluster analysis, which effectively subdivides the broad IPR-based MMF category. For instance, the early Eocene map (Fig. 7A) shows the wide latitudinal spread of Units 2–6 (MMF spectrum), with the more evergreen-rich Units 2 and 3 prevalent in the south, and the conifer-influenced Unit 6 appearing in the north. By the late Eocene (Fig. 7C), a southward contraction of the MMF belt is accompanied by a more pronounced spatial segregation of its subtypes, including the expansion of the more deciduous-rich (Unit 4) and open-canopy (Unit 5) variants in continental interiors.

Zonal vegetation types and their spatial and temporal distribution

Based on established IPR thresholds, six principal zonal vegetation types and two transitional ecotones were identified for the Eocene of East Asia (Table 1). Their spatio-temporal evolution is visualized in Fig. 8. In the early Eocene (Fig. 8A), all vegetation types were present, except ShSF. The period was dominated by MMF (38 floras) and the MMF/BLEF ecotone (14 floras), indicating warm, humid conditions with high plant diversity. The vegetation was overwhelmingly dominated by MMF, which constituted a latitudinally extensive "green belt" from the Arctic (>75°N) to mid-latitudes. This biome was characterized by a balanced mix of broadleaved deciduous (mean ~56.1 %) and evergreen (mean ~20.2 %) taxa (see Figs 3, 4). The MMF/BLEF ecotone and pure BLEF were confined to areas south of ~50°N. BLDF were rare. In the middle Eocene (Fig. 8B), the spectrum of vegetation types simplified, with only BLDF, MMF, BLEF and their ecotones present. MMF remained dominant (39 floras), but a noticeable southward retreat of the MMF/BLEF ecotone is observed compared to the early Eocene. The proportion of evergreen elements within MMF decreased (Fig. 4), while deciduous components slightly increased (Fig. 3), indicating the onset of post-EECO cooling. In the late Eocene (Fig. 8C), MMF (34 floras) persisted as the dominant forest type but with a further increased proportion of deciduous taxa (Fig. 3). This epoch marks the first appearance of ShSF and a more pronounced presence of OWl and Gl/St, particularly in continental interiors.

Synthesis of key spatial and temporal trends

The integrated analysis reveals two primary trends:

1. Latitudinal gradient. Throughout the Eocene, a consistent latitudinal gradient existed: evergreen dominance (BLEF) in the south, a mixed deciduous-evergreen belt (MMF and its ecotones) in the mid-latitudes, and increasing conifer representation (within MMF/BLDF) towards the north. This gradient was remarkably compressed in the early Eocene, with MMF reaching the Arctic.

2. Temporal Evolution. A clear trend of ecological differentiation and provincialization is observed from the early to late Eocene. The homogeneous, evergreen-rich MMF "green belt" of the early Eocene (Figs 2–5, 8A) gradually gave way to a more heterogeneous landscape. By the late Eocene, forests became more deciduous-dominated, and novel, more open biomes (ShSF, OWl, Gl/St) emerged in response to global cooling and increased continentality (Figs 2–5, 8C).

DISCUSSION

Comparative analysis of micro- and macrofloras

Our analysis confirms systematic discrepancies between vegetation reconstructions based on palynological and mac-

Table 1. Trend changes of zonal vegetation components.

Vegetation component	Eocene			Trend
	Early	Middle	Late	
BLE	High proportion	Declining	Low proportion	↓ Strong decline
BLD	Moderate proportion	Increasing	High proportion	↑ Growth
CONIF	Moderate proportion	Stable	Increasing (in high latitudes)	↑ Moderate growth
M-HERB & D-HERB	Low proportion	Emerging	Increasing	↑ Significant growth
ZONPALM & ARBFERN	High proportion (in tropics)	Declining	Low proportion (only in tropics)	↓ Decline

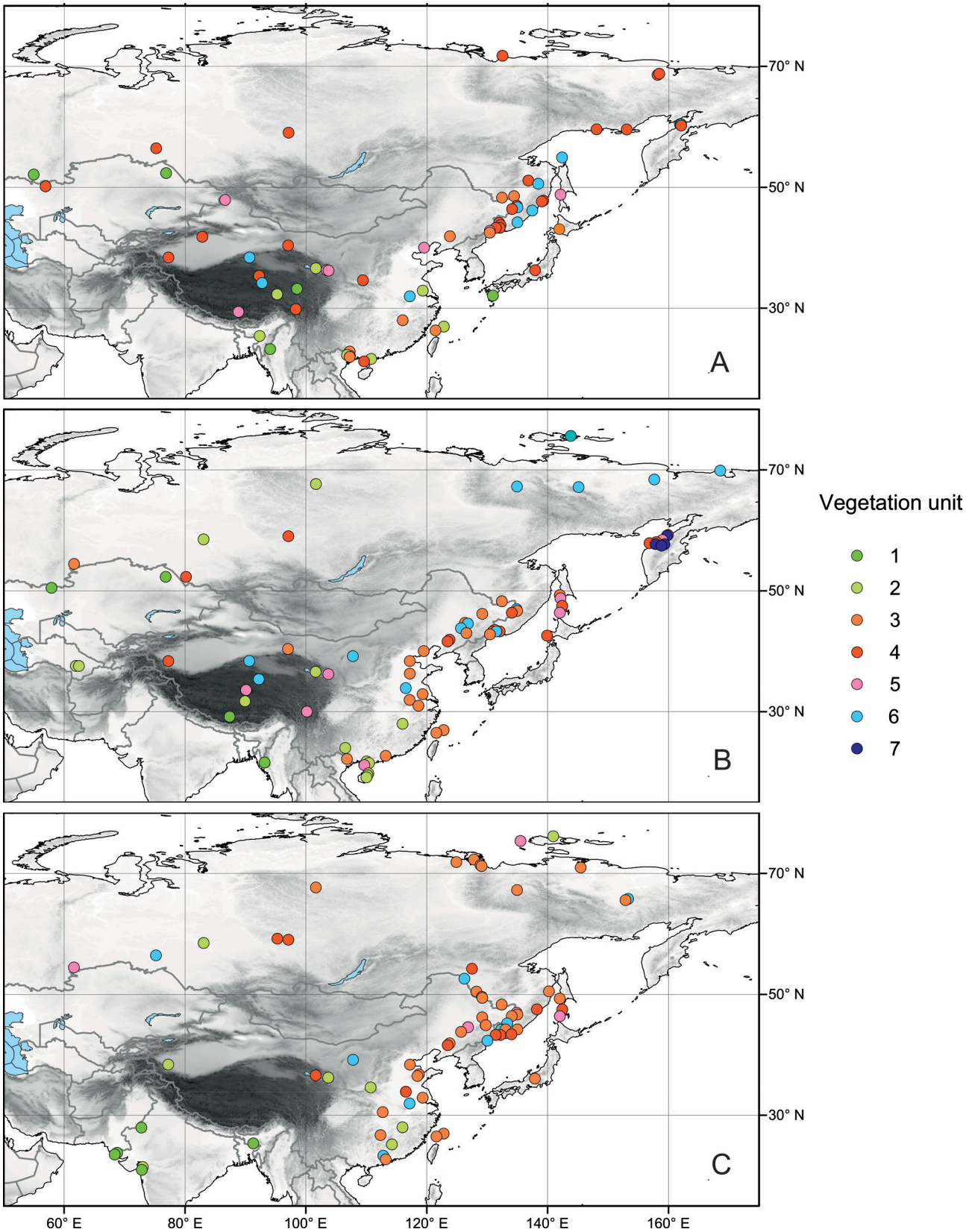

Figure 7 Spatial distribution of the seven floristic groups (Vegetation units 1–7) identified by cluster analysis (see Fig. 6) for the late (A), middle (B), and early (C) Eocene

rofloral data, extending patterns noted in regional studies (Bondarenko et al. 2019, Utescher et al. 2021, Bondarenko & Utescher 2025). These differences stem from fundamental taphonomic and ecological filters, not methodological artefacts of the IPR technique.

Palynofloras provide an integrated signal of regional zonal vegetation due to extensive pollen dispersal and high preservation potential across facies (mean 30.13 zonal taxa per site). In contrast, macroremains (leaves, fruits) predominantly record local, often azonal vegetation (e.g., riparian

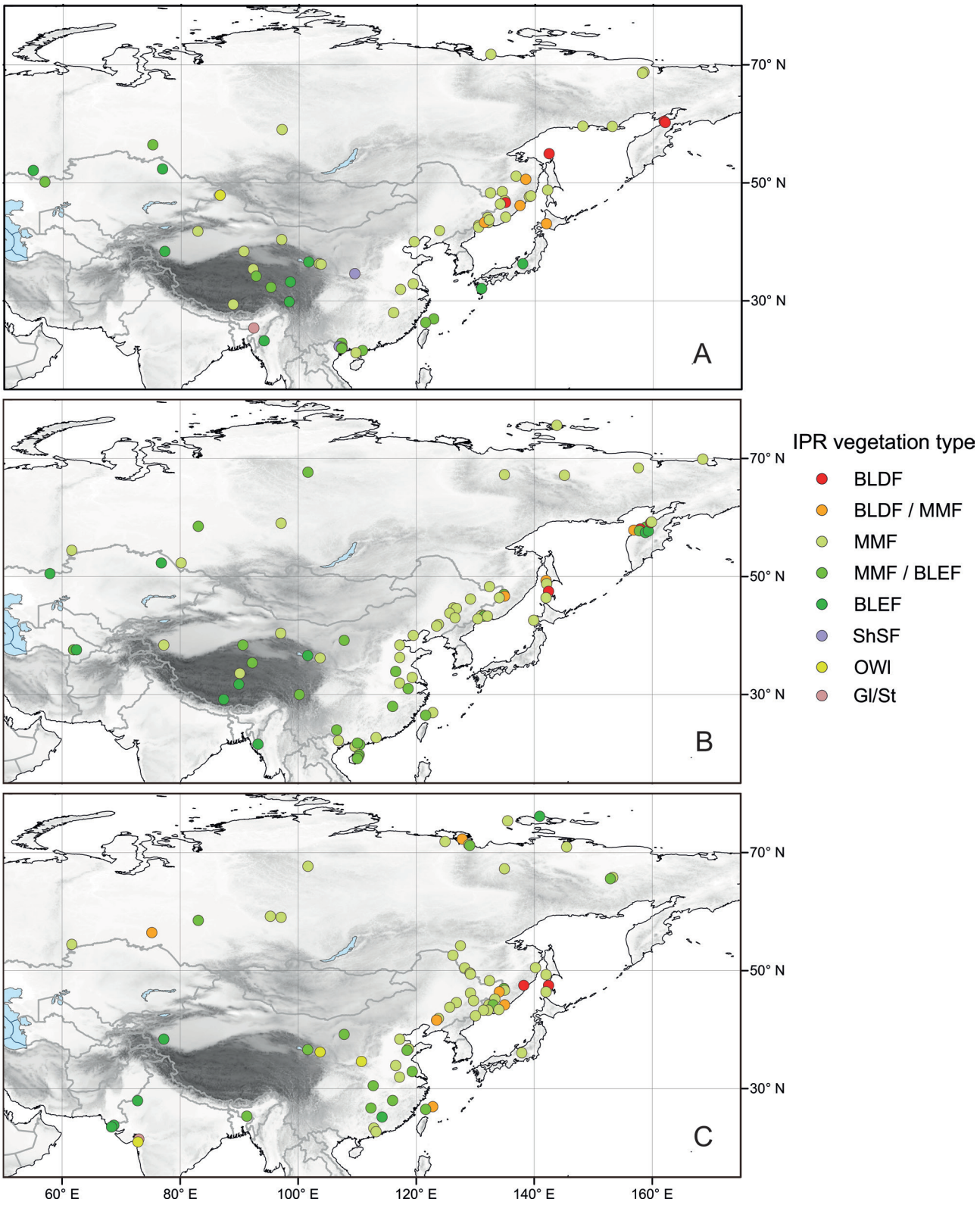

Figure 8 Spatial distribution of vegetation types reconstructed for the late (A), middle (B), and early (C) Eocene

corridors), underrepresenting regional zonal elements (Kovar-Eder & Kvaček 2007). This dichotomy is exemplified at the Erkovtsy locality, where microfloral data indicate a MMF, while the associated macroflora suggests a Gl/St, likely reflecting a local open habitat within a forested landscape.

Furthermore, macrofloras exhibit a taxonomic bias, tending to overrepresent BLD components while underestimating BLE taxa. This is likely not a simple taphonomic artifact related to leaf robustness, as evergreen leaves are often more coriaceous and could be expected to withstand fluvial transport well. Instead, the bias may reflect genuine ecological differences: BLD taxa were likely more frequent in the azonal, riparian vegetation itself (e.g., as fast-growing pioneer plants), which is preferentially captured in macro-

fossil assemblages. Crucially, this apparent "cooling" signal in vegetation structure is not mirrored in quantitative palaeoclimate data from the same floras (Bondarenko & Utescher 2025), highlighting that macrofloras record local community structure under specific edaphic conditions, which can diverge from the regional zonal biome even under identical warm climates.

Therefore, microfloras are superior proxies for reconstructing regional zonal (background) vegetation, while macrofloras excel at capturing its local, often edaphically controlled, variants. This study quantitatively demonstrates the systematic nature of this micro-/macrofloral discrepancy on a continental scale. The analysis of 29 localities with co-occurring micro- and macroremains underscores the integrative value of combined data. Future research should prioritize sections with concurrent preservation of both proxies to minimize taphonomic bias and calibrate more robust vegetation models (Kovar-Eder & Teodoridis 2018).

Dynamics of vegetation components and their palaeoclimatic significance

The proportional representation of IPR zonal components exhibits a consistent latitudinal heterogeneity throughout the Eocene (Figs 2–5). BLD taxa show the greatest range (0–80.5 %) and dominate most floras, particularly at mid-to-high latitudes. BLE components range from 0 to 29.1 %, with their proportion increasing significantly southward, forming a distinct latitudinal cline (Fig. 4). CONIF range from 0 to 23.5 %, showing a pronounced increase towards the Arctic, indicating cooler conditions (Fig. 2). SCL+LEG components are consistently rare (<5 %), except in a few late Eocene sites. ZONPALM and ARBFERN are primarily present in early Eocene low-latitude records (Fig. 5), highlighting peak warmth. This spatial pattern serves as a direct vegetation proxy for the palaeotemperature gradient, with the southward increase in BLE correlating with higher mean annual and winter temperatures (Bondarenko & Utescher 2022, Li et al. 2022).

A clear temporal trend marks the transition from the early to late Eocene, reflecting global climatic evolution (Table 1). The early Eocene, characterized by the EECO, exhibits the highest proportions of thermophilic elements (high BLE, common ZONPALM/ARBFERN in the south). The middle Eocene marks the onset of post-EECO cooling, with a noticeable decline in BLE proportions (Fig. 4) and a slight increase in BLD components (Fig. 3), signalling a shift towards greater deciduousness. The late Eocene saw significant ecological differentiation: a further increase in BLD (Fig. 3), expansion of herbaceous components (D-HERB & M-HERB) (Fig. 5, Table 1), and a more pronounced presence of non-forest biomes. This trend correlates with increased climatic seasonality and the onset of regional aridification linked to global cooling (Zachos et al. 2008, Bosboom et al. 2014).

Based on the proportions of zonal components, a dense forest cover existed at most Eocene sites. Trees constituted the dominant life form (Fig. 5), averaging over 80 % of zonal components, with high diversities (70–80 %) even at high latitudes (55–75°N), consistent with previous reconstructions. Multiple studies have indicated the prevalence of forest vegetation (Grinenko et al. 1989, Fradkina 1995, Kodrul 1999, Suan et al. 2017, Bondarenko et al. 2019, 2022, 2024a, Li et al. 2022 [for eastern and southeastern sites only], Xie et al. 2022, Bondarenko & Utescher 2023, 2024b, 2025, etc.). Herbaceous life forms were predominantly represented by hygrophilous pteridophytes (M-HERB), while angiosperm herbs were rare, aligning with data for Paleogene records (Utescher & Mosbrugger 2007, Bondarenko & Utescher 2024b) and coinciding with reconstructed high humidity throughout the Eocene of East Asia (Bondarenko & Utescher 2023, Bondarenko 2025)

The dominant Mixed Mesophytic Forest (MMF) biome and forest openness

The most salient feature of Eocene vegetation in Asia is the ubiquity of the MMF biome, identified in 111 of the 211 analyzed floras (Table 2). This unique paleo-biome, lacking a precise modern analogue, was characterized by a remarkably balanced and diverse mix of BLD (44.3–77.6 %) and BLE (14.9–29.9 %) angiosperm taxa, often with a conifer understory or admixture. Its latitudinal range, extending unbroken to high Arctic latitudes (>75°N) (Table 3), serves as a robust biogeographic proxy for an extremely weak meridional temperature gradient and persistently ice-free poles during the EECO and subsequent greenhouse conditions (Zachos et al. 2001, Westerhold et al. 2020).

Our quantitative data refine earlier conceptual models. They corroborate the hypothesis of weakly differentiated, relatively uniform mesophytic vegetation across high northern latitudes (Akhmetiev 2004, Aleksandrova et al. 2015) and align with recent high-resolution Arctic reconstructions based on megafloral analysis, which describe species-rich, broadleaved deciduous–evergreen communities (Golovneva et al. 2023). Crucially, the significant proportion of BLD taxa within Arctic MMF assemblages contradicts classical models that proposed paratropical or subtropical rainforests (e.g., the "Megathermal" biome of Wolfe 1985) at these latitudes. Instead, it indicates the presence of a distinct, albeit warm, seasonality – likely photoperiodically forced – that favoured deciduousness as an adaptive strategy to a light-limited winter dark season (Spicer et al. 2019). This observation supports the concept of BLDF for high latitudes proposed by Collinson & Hooker (2003). However,

Table 2. Identified zonal vegetation types for the Eocene of East Asia, their key characteristics, and frequency.

Vegetation type	Key characteristics	Number of floras
MMF	CONIF: 0–46.4%, BLD: 44.3–77.6%, BLE: 14.9–29.9%	111
BLEF	BLE > 40%	24
BLDF	CONIF: 9.9–42.9%, BLD: 80.6–100%	11
OWl	High herb proportion (31.1–33.7%)	4
ShSF	High SCL+LEG (22.2–26.6%)	2
St/Gl	Dominant herbs (55.1–56.3%)	2
MMF/BLEF	Intermediate between MMF and BLEF	45
BLDF/MMF	Intermediate between BLDF and MMF	12

our analysis necessitates a crucial amendment: the consistent and substantial evergreen admixture justifies classifying these high-latitude ecosystems as a subtype of MMF. This classification highlights their inherently transitional, "mixed" nature, representing a stable biome under Paleogene greenhouse conditions rather than a simple latitudinal extension of modern boreal or nemoral forests.

Superimposed on this overarching MMF dominance, a clear latitudinal gradient in floristic composition existed, which is quantitatively resolved by the cluster analysis (Table 4, Figs 6, 7). The southward monotonic increase in the BLE component is reflected in the transition from conifer-influenced (Unit 6) and deciduous-rich (Unit 4) MMF subtypes at higher latitudes, through the core MMF groups with balanced evergreen admixture (Units 3 and 2), culminating in a well-defined MMF/BLEF ecotone and pure BLEF (Unit 1) south of approximately 50°N (Fig. 7). This structured gradient, revealed by the clustering, directly correlates with increasing mean annual temperature (MAT) and cold month mean temperature (CMMT) (Bondarenko & Utescher 2022, Bondarenko et al. 2024b). This pattern is in strong agreement with quantitative PFT (Li et al. 2022) and Climate-Leaf Analysis Multivariate Program (CLAMP) analyses (Spicer et al. 2021) from the Eocene of China, which reconstruct a steepening temperature gradient from the EECO into the middle Eocene.

A critical finding of our study concerns forest openness and aridity. Truly open, non-forest vegetation types – such as OWl and Gl/St – were extremely rare throughout most of the Eocene, appearing sporadically and with low taxonomic diversity only in the early and late Eocene. Similarly, ShSF were limited to just two late Eocene floras (Table 2).

This pattern critically addresses the long-standing debate on Eocene Asian aridity. The very low representation of SCL and LEG components in our continent-wide synthesis contradicts models proposing a simple, continuous zonal arid belt stretching across interior Asia (e.g., Zhang et al. 2012). Our data reveal a more nuanced picture. While evidence for localized, seasonal aridity exists, it does not equate to continent-wide desertification during the early to middle Eocene. For instance, palynological studies from the Hengyang Basin in southern China (Hunan Province) report a high abundance of xerophytic shrubs (e.g., *Nitrariadites*, *Ephedripites*) and a notable scarcity of humid forest pollen during the early Eocene, interpreted as evidence for a desert environment (Xie et al. 2020). However, this site represents a specific, likely basin-controlled, paleoenvironment. Its signal is not representative of the broader latitudinal belt, as demonstrated by our synthesis and by other records from similar latitudes in China that show fully forested conditions (e.g., Li et al. 2022).

This apparent contradiction highlights the importance of a mosaic landscape model (Bosboom et al. 2014, Sun et al. 2022). In this model, lithological evidence for episodic aridity (e.g., evaporites, red beds) and isolated palynological records of xerophytic dominance reflect localized moisture deficits within otherwise forested continents. These could occur in rain shadows of nascent uplands, in interior basins with restricted atmospheric moisture recycling, or in areas with specific edaphic conditions. The transient development of a south subtropical forest ecosystem in central China during the peak of the Paleocene–Eocene Thermal Maximum (PETM), as evidenced by a brief spike in humid-tolerant pollen (Xie et al. 2022), further underscores the dynamic and patchy nature of Eocene landscapes, where vegetation responded rapidly to short-term hyperthermal events within a generally warm and humid background state.

Our continent-scale reconstruction, showing the overwhelming dominance of forest biomes, aligns with the most recent global syntheses. A new global vegetation model-data comparison for the early Eocene confirms that forest cover was extensive worldwide, with arid and open biomes occupying less than 10 % of the land surface and being largely confined to localized continental interiors and lee sides of major topographic features (Thompson et al. 2025). Therefore, the Eocene landscape of Asia is best understood not as an arid belt, but as a forested continent punctuated by scattered, seasonally dry basins or xeric patches, with significant, widespread aridification being a hallmark of the late Eocene to Oligocene transition (Barbolini et al. 2020, Carrapa et al. 2022).

Table 3. Geographic zonation in the late Eocene (based on Figs 2–5).

Latitudinal zone	Dominant zonal vegetation component	Additional zonal vegetation component
High (>50°N)	CONIF + BLD	ZONHERB
Mid (30–50°N)	BLD	CONIF, ZONHERB
Low (<30°N)	BLE	ZONPALM, ARBREFN (limited)

Table 4. Spatiotemporal trends of vegetation changes (based on Figs. 2–5, 8).

Region	Eocene			Trend
	Early	Middle	Late	
High latitudes (45–60°N)	MMF, BLDF	BLDF, MMF	BLDF, conifers	Strengthening the role of deciduous and coniferous trees
Mid-latitudes (30–45°N)	MMF, MMF/BLEF	MMF, BLDF/MMF	MMF, OWl, St/Gl	Cooling, increased seasonality, aridization
Low latitudes (20–30°N)	BLEF, palms & tree ferns	BLEF, MMF/BLEF	BLEF, ShSF	Stable warmth, but increasing aridity
Highlands/inland areas	MMF, OWl	MMF	OWL, St/Gl, ShSF	Formation of arid and mountain biomes

Reconstructed vegetation patterns: biome dynamics and spatial evolution

The reconstructed latitudinal vegetation zonation serves as a powerful, direct terrestrial proxy for the meridional temperature gradient during the Eocene. The unprecedented poleward extension of the MMF biome into the high Arctic (>75°N) provides robust biogeographic evidence for an extremely weak temperature gradient. This is a critical terrestrial validation of the "equable" greenhouse climate, where polar amplification of warmth resulted in high-latitude winters that were largely frost-free (Jahren & Sternberg 2008). Our data are quantitatively consistent with marine proxy records (e.g., TEX86, $\delta^{18}O$) that indicate polar sea surface temperatures (SSTs) exceeding 15–20°C during the EECO (Zachos et al. 2001, Sluijs et al. 2006). Furthermore, this vegetation pattern aligns with the predictions of state-of-the-art paleoclimate models (e.g., Farnsworth et al. 2019, Lunt et al. 2021), which simulate a reduced equator-to-pole temperature gradient of roughly half its modern value under high pCO_2 conditions. The presence of a significant evergreen component within these high-latitude forests imposes a critical constraint, indicating that CMMT likely remained above 5°C, preventing large-scale winter defoliation (Spicer et al. 2021).

The temporal evolution of Asian biomes from the early to late Eocene provides direct ecological evidence for the continent's response to major, stepwise global climatic shifts. The early Eocene vegetation homogeneity, characterized by the expansive MMF/BLEF "green belt," mirrors the peak warmth and low temperature seasonality of the EECO (ca. 53–49 Ma) (Westerhold et al. 2020). The subsequent transition towards more deciduous-dominated forests in the middle Eocene is a direct ecological fingerprint of post-EECO cooling. This is particularly evident in the southward retreat of the MMF/BLEF ecotone and the reduced proportion of BLE taxa within MMF, which correlate with a global drop in bottom-water temperatures and high-latitude cooling of ~4–6°C (Zachos et al. 2008, Bijl et al. 2013). Our vegetation data thus capture the terrestrial biome's sensitivity to even moderate global temperature change, with deciduousness serving as a key adaptive response to increased climatic seasonality and/or cooler winter temperatures.

The late Eocene marks a pivotal climatic-vegetational transition. The first consistent appearance sclerophyllous (ShSF) and a more pronounced presence of open (OWl, Gl/St) vegetation types, particularly in the continental interiors of Central Asia, is not a random event but a signature of profound atmospheric and tectonic reorganization. This diversification correlates strongly with two interconnected processes: 1) the global shift towards an "icehouse" climate following the Middle Eocene Climatic Optimum (MECO) and the growth of Antarctic ice sheets (Bohaty et al. 2009), and 2) the regional inception and intensification of the Asian monsoon-arid system.

Our vegetation mosaic model offers a concrete, testable ecological scenario for this critical transitional period (~41–34 Ma). The development of ShSF and open patches within a still-dominant forest matrix reflects the onset of increased precipitation seasonality – a hallmark of monsoon circulation – coupled with overall aridification. This aligns with isotopic ($\delta^{18}O$, $\delta^{13}C$) and sedimentological evidence from basins across Asia (e.g., Xining, Junggar, Tarim) that indicate a major shift towards drier conditions and enhanced seasonality around the Eocene–Oligocene transition (Bosboom et al. 2014, Yuan et al. 2020, Sun et al. 2022). The retreat of the Paratethys Sea from Central Asia during this period was likely a key driver, reducing a major moisture source and increasing continentality (Ramstein et al. 1997, Zhang et al. 2007). Concurrently, the initial topographic growth of the Tibetan Plateau and the Himalayan orogen began to dynamically alter atmospheric circulation, potentially enhancing rain-shadow effects in the interior and strengthening seasonal wind patterns (Guo et al. 2002, Licht et al. 2014).

Therefore, the late Eocene vegetation shift documented here – from homogeneous, humidity-loving forests to a differentiated mosaic including seasonally dry and open biomes – represents the direct terrestrial ecological manifestation of the coupled global cooling and regional tectonic forces that ultimately established the modern pattern of Asian climate and biomes. It underscores that the stage for the continent's iconic arid interior was set not in the Miocene, but during the climatic upheavals of the late Eocene.

CONCLUSIONS

Application of the Integrated Plant Record (IPR) analysis to 240 Eocene floras from across Asia has enabled a robust reconstruction of zonal vegetation dynamics throughout the epoch, providing a comprehensive continental-scale synthesis.

The defining feature of the Eocene Asian landscape was the latitudinally extensive dominance of Mixed Mesophytic Forests (MMF). This unique biome, characterized by a balanced mix of broadleaved deciduous and evergreen taxa, has no direct modern analogue. Its extension into the high Arctic (>75°N) serves as a key biogeographic indicator of an extremely weak meridional temperature gradient during the early Paleogene greenhouse climate.

A clear latitudinal vegetation gradient persisted throughout the Eocene, driven primarily by temperature. The proportion of broadleaved evergreen (BLE) components increased systematically southward, forming a distinct MMF/Broadleaved Evergreen Forest (BLEF) ecotone, with pure BLEF confined to areas south of approximately 50°N.

The evidence for aridity in central continental Asia, primarily derived from lithological proxies, is reconciled with the forest-dominated palynological record through a mosaic landscape model. We conclude that the environment was not characterized by a continuous zonal desert but rather comprised a mosaic of seasonally dry forests interspersed with localized open, xerophytic patches – an interpretation supported by regional high-resolution studies.

A significant temporal trend of increasing ecological differentiation and provincialization is identified from the early to the late Eocene. The homogeneous, warm, and humid conditions of the early Eocene, marked by the dominance of MMF, gradually gave way to a more heterogeneous land-

scape. The late Eocene marks the continent-wide onset of aridification, evidenced by the first appearance of Subhumid Sclerophyllous Forests (ShSF) and a more pronounced presence of open vegetation types (OWl, Gl/St), correlating with post-Early Eocene Climatic Optimum (EECO) cooling and increased seasonality.

Systematic discrepancies between vegetation reconstructions based on micro- (palynological) and macrofloral (leaf, fruit) data are documented and attributed to fundamental taphonomic and ecological filters. This underscores the necessity of interpreting these records as complementary: palynological data best reflect the regional zonal vegetation, while macrofloras primarily capture local, often edaphically controlled habitat conditions.

This continental-scale synthesis quantitatively validates and refines existing regional models. It confirms the early Paleogene "green belt" of MMF along the Pacific margin of Eurasia and pinpoints the late Eocene as the critical starting point for the biome differentiation that ultimately led to Asia's modern, highly contrasting vegetation pattern

ACKNOWLEDGEMENTS

The research was carried out within the state assignment of Ministry of Science and Higher Education of the Russian Federation (theme No. 124012200182-1). This work is a contribution to NECLIME (the research Network on Cenozoic Climate and Ecosystems).

LITERATURE CITED

Akhmetiev, M.A. 2004. The Paleocene and Eocene global climate. Paleobotanical evidences. In: *Climate in the epoches of major biospheric transformations (Trudy Geologicheskogo Instituta RAN, Vol. 550)* (M.A. Semikhatov & N.M. Chumakov, eds), pp. 10–43, Geologicheskii institute RAN, Moscow (in Russian). [Ахметьев М.А. 2004. Климат земного шара в палеоцене и эоцене по данным палеоботаники // Климат в эпохи крупных биосферных перестроек (Труды ГИН РАН. Вып. 550) / под ред. М.А. Семихатова, Н.М. Чумакова. Москва: ГИН РАН. С. 10–43].

Aleksandrova, G.N., T.M. Kodrul & J.-H. Jin 2015. Palynological and paleobotanical investigations of Paleogene sections in the Maoming basin, South China. *Stratigraphy and Geological Correlation* 23(3):300–325.

Amon, E.O. 2001. Marine areas of the Ural region in the Middle and Late Cretaceous. *Geologiya i Geofizika* 42(3):471–483. [Амон Э.О. 2001. Морские акватории Уральского региона в средне- и позднемеловое время // Геология и геофизика. Т. 42, № 3. С. 471–483].

Amon, E.O. 2018. Factors and conditions of accumulation of biogenic silicites in the Paleogene basin of Western Siberia. *Byulleten' Moskovskogo obshchestva ispytatelei pripody. Otdel geologicheskii* 93(4):51–67. [Амон Э.О. 2018. Факторы и условия накопления биогенных силицитов в палеогеновом бассейне Западной Сибири // Бюллетень МОИП. Отд. геол. Т. 93, № 4. С. 51–67].

Barbolini, N., A. Woutersen, D. Silvestro, D. Tardif, N. Meijer, C. Dionisic, A. Rohrmann, A. Licht, H. Custard, C. Hoorn & S.G.A. Flantua 2020. Cenozoic evolution of the steppe-desert biome in Central Asia. *Science Advances* 6(41):eabb8227.

Bijl, P.K., J.A. Bendle, S.M. Bohaty, J. Pross, S. Schouten, L. Tauxe, C.E. Stickley, R.M. McKay, U. Röhl, M. Olney, A. Sluijs, C. Escutia Dotti, H. Brinkhuis & Expedition 318 scientists 2013. Sea surface temperature based on TEX86 as well as mean annual air temperature based on CBT and MBT from ODP Hole 189-1172A [dataset]. PANGAEA, https://doi.org/10.1594/PANGAEA.816364. In supplement to: *Eocene cooling linked to early flow across the Tasmanian Gateway* (P.K. Bijl et al.). *Proceedings of the National Academy of Sciences of the United States of America* 110(24):9645–9650.

Bohaty, S.M., J.C. Zachos, F. Florindo & M.L. Delaney 2009. Coupled greenhouse warming and deep-sea acidification in the middle Eocene. *Paleoceanography* 24(2):PA2207.

Bondarenko, O.V. 2025. Plants as a proxy for monsoon reconstruction – a case study from the Eocene of East Asia. *Earth History and Biodiversity* 6:100035.

Bondarenko, O.V. & T. Utescher 2022. Early Paleogene continental temperature patterns and gradients over eastern Eurasia. *Journal of Asian Earth Sciences* 239:105401.

Bondarenko, O.V. & T. Utescher 2023. Late early to early middle Eocene climate and vegetation change at Tastakh Lake (northern Yakutia, Eastern Siberia). *Palaeobiodiversity and Palaeoenvironments* 103(2):277–301.

Bondarenko, O.V. & T. Utescher 2024a. Early Paleogene precipitation patterns over East Asia: Was there a monsoon after all? *Palaeobiodiversity and Palaeoenvironments* 104(1):1–28.

Bondarenko, O.V. & T. Utescher 2024b. Early Paleogene vegetation units of East Asia and their spatial distribution. *Palaeogeography, Palaeoclimatology, Palaeoecology* 639:112064.

Bondarenko, O.V. & T. Utescher 2025. Early Paleogene plant biomes of the Pacific side of Eurasia. *Palaeoworld* 34(1):100865.

Bondarenko, O.V., N.I. Blokhina, T.A. Evstigneeva & T. Utescher 2022. Short-term climate and vegetation dynamics in Lena River Delta (northern Yakutia, Eastern Siberia) during early Eocene. *Palaeoworld* 31(3):521–541.

Bondarenko, O.V., N.I. Blokhina & T. Utescher 2019. Major plant biome changes in the Primorye Region (Far East of Russia) during the Paleogene. *Botanica Pacifica* 8(1):3–18.

Bondarenko, O.V., T.A. Evstigneeva, R.Z. Allaguvatova, A.A. Zhmerenetsky & T. Utescher 2024a. Reconstruction of zonal vegetation of East Asia in the early Eocene. *Biota i sreda prirodnykh territorii* 12(1):5–22 (in Russian). [Бондаренко О.В., Евстигнеева Т.А., Аллагуватова Р.З., Жмеренецкий А.А., Утешер Т. 2024а. Реконструкция зональной растительности востока Азии в раннем эоцене // Биота и среда природных территорий. Т. 12, № 1. С. 5–22].

Bondarenko, O.V., T.A. Evstigneeva, A.A. Zhmerenetsky, R.Z. Allaguvatova & T. Utescher 2024b. Spatial reconstruction of the East Asia climate in the early Eocene. *Vestnik Severo-Vostochnogo nauchnogo centra DVO RAN* 1:14–25. [Бондаренко О.В., Евстигнеева Т.А., Жмеренецкий А.А., Аллагуватова Р.З., Утешер Т. 2024. Пространственная реконструкция климата востока Азии в раннем эоцене // Вестник Северо-Восточного научного центра ДВО РАН. № 1. С. 14–25].

Bosboom, R.E., H.A. Abels, C. Hoorn, B.C.J. van den Berg, Z. Guo & G. Dupont-Nivet 2014. Aridification in continental Asia after the Middle Eocene Climatic Optimum (MECO). *Earth and Planetary Science Letters* 389:34–42.

Burke, K.D., J.W. Williams, M.A. Chandler, A.M. Haywood, D.J. Lunt & B.L. Otto-Bliesner 2018. Pliocene and Eocene provide best analogs for near-future climates. *Proceedings of the National Academy of Sciences of the United States of America* 115(52):13288–13293.

Carrapa, B., P.G. DeCelles, P. Zhang, M. Harrison, J. Ding, G. Gehrels, L. Li, G. Zhuang & P. Kapp 2022. Orogenic

wedge evolution and climate change in the late Eocene to early Oligocene, Central Tibet. *Geology* 50(6):654–658.

Cohen, K.M., S.C. Finney, P.L. Gibbard & J.-X. Fan 2013. The ICS International Chronostratigraphic Chart. *Episodes* 36(3):199–204.

Collinson, M.E. 2000. Cenozoic evolution of modern plant communities and vegetation. In: *Biotic response to global change: The last 145 million years* (S.J. Culver & P.F. Rawson, eds), pp. 223–243, Cambridge University Press, Cambridge.

Collinson, M.E. & J.J. Hooker 2003. Paleogene vegetation of Eurasia: framework for mammalian faunas. *Deinsea* 10:41–83.

Farnsworth, A., D.J. Lunt, C.L. O'Brien, G.L. Foster, G.N. Inglis, P. Markwick, R.D. Pancost & S.A. Robinson 2019. Climate sensitivity on geological timescales controlled by nonlinear feedbacks and ocean circulation. *Geophysical Research Letters* 46(16):9880–9889.

Fradkina, A.F. 1995. *Palynostratigrapy of Paleogene and Neogene sediments of North-Eastern Russia (Transactions of the UIGGM SB RAS, Vol. 806)*. Nauchno-izdatel'skii tsentr OIGGiM SO RAN, Novosibirsk, 82 pp. (in Russian). [Фрадкина А.Ф. 1995. Палиностратиграфия палеогеновых и неогеновых отложений Северо-Востока России (Труды ОИГГМ СО РАН, Вып. 806). СО РАН: Новосибирск, 82 с.].

Gladenkov, Yu.B., O.K. Bazhenova, V.I. Grechin, L.S. Margulis & B.A. Salnikov 2002. The Cenozoic geology and the oil and gas presence in Sakhalin. GEOS, Moscow, 225 pp. (in Russian). [Гладенков Ю.Б., Баженова О.К., Гречин В.И., Маргулис Л.С., Сальников Б.А. 2002. Геология кайнозоя и нефтегазоносность Сахалина. Москва: ГЕОС. 225 с.].

Gladenkov, Yu.B., V.N. Sinelnikova, A.I. Chelebaeva & A.E. Shantser 2005. *Biosphere–ecosystem–biota in the Earth past. The North Pacific Cenozoic ecosystems: Eocene–Oligocene of west Kamchatka and adjacent regions (To the Centenary of Academician V.V. Menner). (Trudy Geologicheskogo Instituta RAN 540)*. GEOS, Moscow, 480 pp. (in Russian). [Гладенков Ю.Б., Синельникова В.Н., Челебаева А.И., Шанцер А.Е. 2005. Биосфера–Экосистема–Биота в прошлом Земли. Северотихоокеанские кайнозойские экосистемы: эоцен–олигоцен Западной Камчатки и сопредельных регионов (К 100-летию со дня рождения академика В.В. Меннера). (Труды Геологического института РАН 540). Москва: ГЕОС. 480 с.].

Golovneva, L.B., A.A. Zolina & R.A. Spicer 2023. The early Paleocene (Danian) climate of Svalbard based on palaeobotanical data. *Papers in Palaeontology* 9(2):e1533.

Greenwood, D.R. & S.L. Wing 1995. Eocene continental climates and latitudinal temperature gradients. *Geology* 23(11):1044–1048.

Grinenko, O.V., A.I. Sergeenko & I.N. Belolubskiy 1997. Stratigraphy of the Paleogene and Neogene deposits of the North-East of Russia. *Otechestvennaya Geologiya* 8:14–20 (in Russian). [Гриненко О.В., Сергеенко А.И., Белолюбский И.Н. 1997. Стратиграфия палеогеновых и неогеновых отложений Северо-Востока России // Отечественная геология. № 8. С. 14–20].

Grinenko, O.V., L.P. Zharikova, A.F. Fradkina et al. 1989. *The Paleogene and Neogene of the North-Eastern USSR*. Yakut Scientific Center SO AN USSR, Yakutsk, 184 pp. [Гриненко О.В., Жарикова Л.П., Фрадкина А.Ф. и др. 1989. Палеоген и неоген Северо-Востока СССР. Якутск: ЯНЦ СО АН СССР. 184 с.].

Guo, Z.T., W.F. Ruddiman, Q.Z. Hao, H.B. Wu, Y.S. Qiao, R.X. Zhu, S.Z. Peng, J.J. Wei, B.Y. Yuan & T.S. Liu 2002. Onset of Asian desertification by 22 Myr ago inferred from loess deposits in China. *Nature* 416(6877):159–163.

Hammer, Ø., D.A.T. Harper & P.D. Ryan 2001. PAST: Paleontological statistics software package for education and data analysis. *Palaeontologia Electronica* 4(1):9.

Herman, A., R.A. Spicer, G.N. Aleksandrova, J. Yang, T. Kodrul, N.P. Maslova, T.E.V. Spicer, G. Chen & J.-H. Jin 2017. Eocene – Early Oligocene climate. *Cretaceous Research* 69:91–114.

Huang, Y.-J., Y.-F. Wang & C.-S. Li 1998. Paleocene flora from the Wuyun Formation in Jiayin of Heilongjiang, China. *Acta Palaeontologica Sinica* 37(2):249–256 (in Chinese with English abstract).

Jahren, A.H. & L.S.L. Sternberg 2008. Annual patterns within tree rings of the Arctic middle Eocene (ca. 45 Ma): Isotopic signatures of precipitation, relative humidity, and deciduousness. *Geology* 36(2):99–102.

Kezina, T.V. 2005. *Palynostratigraphy of coal deposits of the Late Cretaceous and Cenozoic of the Upper Amur River region*. Dal'nauka, Vladivostok, 206 pp. (in Russian). [Кезина Т.В. 2005. Палиностратиграфия угленосных отложений позднего мела и кайнозоя Верхнего Приамурья. Владивосток: Дальнаука. 206 с.].

Kodrul, T.M. 1999. *Paleogene phytostratigraphy of South Sakhalin (Transaction of the Geological Institute RAS, Vol. 519)*. Nauka, Moscow, 150 pp. (in Russian). [Кодрул Т.М. 1999. Фитостратиграфия палеогена южного Сахалина (Труды Геологического института РАН, вып. 519). Москва: Наука. 164 с.].

Kovar-Eder, J. & Z. Kvaček 2003. Towards vegetation mapping based on the fossil plant record. *Acta Universitatis Carolinae, Geologica* 46(4):7–13.

Kovar-Eder, J. & Z. Kvaček 2007. The integrated plant record (IPR) to reconstruct Neogene vegetation: the IPR-vegetation analysis. *Acta Palaeobotanica* 47(2):391–418.

Kovar-Eder, J. & V. Teodoridis 2018. The middle Miocene central European plant record revisited; widespread subhumid sclerophyllous forests indicated. *Fossil Imprint* 74(1–2):115–134.

Kovar-Eder, J., H. Jechorek, Z. Kvaček & V. Parashiv 2008. The Integrated Plant Record: an essential tool for reconstructing Neogene zonal vegetation in Europe. *Palaios* 23(2):97–111.

Krestov, P.V. 2006. *Vegetation cover and phytogeographic lines of the Northern Pacific*. PhD. Thesis. Vladivostok, 42 pp. (in Russian). [Крестов П.В. 2006. Растительный покров и фитогеографические линии Северной Пацифики. Автореферат ... докт. биол. наук. Владивосток, 42 с.].

Li, Q.J., T. Utescher, Y.S.C. Liu, D. Ferguson, H. Jia & C. Quan 2022. Monsoonal climate of East Asia in Eocene times inferred from an analysis of plant functional types. *Palaeogeography, Palaeoclimatology, Palaeoecology* 601:111138.

Li, Y.T. 1984. *The Tertiary system of China*. Beijing: Geological Publishing House (in Chinese).

Licht, A., M. van Cappelle, H.A. Abels, J.-B. Ladant, J. Trabucho-Alexandre, C. France-Lanord, Y. Donnadieu, J. Vandenberghe, T. Rigaudier, ... & J.-J. Jaeger 2014. Asian monsoons in a late Eocene greenhouse world. *Nature* 513(7519):501–506.

Lunt, D.J., F. Bragg, W.-L. Chan, D.K. Hutchinson, J.-B. Ladant, P. Morozova, I. Niezgodzki, S. Steinig, Z. Zhang, ... & B.L. Otto-Bliesner 2021. DeepMIP: model intercomparison of early Eocene climatic optimum (EECO) large-scale climate features and comparison with proxy data. *Climate of the Past* 17(1):203–227.

Miao, Y., X. Fang, C. Song, X. Yan, P. Zhang, Q. Meng, J. Li & F. Wu 2008. Late Cenozoic climate change in the Linxia Basin (NE Tibetan Plateau): Evidence from clay minerals. *Palaeogeography, Palaeoclimatology, Palaeoecology* 260(1–2):122–131.

Pavlutkin, B.I. & T.I. Petrenko 2010. *Stratigraphy of Paleogene–Neogene sediments in Primory'e*. Dal'nauka, Vladivostok. 164 pp. (in Russian). [Павлюткин Б.И., Петренко Т.И. 2010. Стратиграфия палеоген–неогеновых отложений Приморья. Владивосток,: Дальнаука. 164 с.].

Pei, J., Z. Sun, X. Wang, Y. Zhao, X. Ge, X. Guo, H. Li & J. Si 2009. Evidence for Tibetan Plateau uplift in Qaidam Basin before Eocene–Oligocene boundary and its climatic implications. *Journal of Earth Science* 20(5):430–437.

Pound, M.J., A.M. Haywood, U. Salzmann & J.B. Riding 2012. Global vegetation dynamics and latitudinal temperature gradients during the Mid to Late Miocene (15.97–5.33 Ma). *Earth-Science Reviews* 112(1–2):1–22.

Quan, C., Y.S.C. Liu & T. Utescher 2012. Eocene monsoon prevalence over China: A palaeobotanical perspective. *Palaeogeography, Palaeoclimatology, Palaeoecology* 365–366:302–311.

Ramstein, G., F. Fluteau, J. Besse & S. Joussaume 1997. Effect of orogeny, plate motion and land–sea distribution on Eurasian climate change over the past 30 million years. *Nature* 386(6627):788–795.

Salzmann, U., A.M. Haywood & D.J. Lunt 2009. The past is a guide to the future? Comparing Middle Pliocene vegetation with predicted biome distributions for the twenty-first century. *Philosophical Transactions of the Royal Society A: Mathematical, Physical and Engineering Sciences* 367(1886): 189–204.

Shi, F., X.-R. Zhang, Z.-J. Liu, H.-Y. Wang & J.-G. Yang 2008. Thrust event of the provenances revealed by zircon fission track ages in Tangyuan Fault-Basin, NE China. *Radiation Measurements* 43(1):S324–S328.

Sluijs, A., S. Schouten, M. Pagani, M. Woltering, H. Brinkhuis, J.S.S. Damsté, G.R. Dickens, M. Huber, G.-J. Reichart, ... & the Expedition 302 Scientists. 2006. Subtropical Arctic Ocean temperatures during the Palaeocene/Eocene thermal maximum. *Nature* 441(7093):610–613.

Spicer, R.A., P.J. Valdes, A. Hughes, J. Yang, T.E.V. Spicer, A.B. Herman & A. Farnsworth 2019. New insights into the thermal regime and hydrodynamics of the early Late Cretaceous Arctic. *Geological Magazine* 156(5):721–741.

Spicer, R.A., T. Su, P.J. Valdes, A. Farnsworth, F.-X. Wu, G. Shi, T.E.V. Spicer & Z.-K. Zhou 2021. Why 'the uplift of the Tibetan Plateau' is a myth. *National Science Review* 8(1):nwaa091.

Suan, G., S.-M. Popescu, J.-P. Suc, J. Schnyder, S. Fauquette, F. Baudin, D. Yoon, K. Piepjohn, N.N. Sobolev & L. Labrousse 2017. Subtropical climate conditions and mangrove growth in Arctic Siberia during the early Eocene. *Geology* 45(6):539–542.

Sun, J., D.J. Lunt, Z. Zhang & M. Vahlenkamp 2022. Evolution of continental temperature seasonality from the Eocene greenhouse to the Oligocene icehouse – a model–data comparison. *Climate of the Past* 18(2):341–367.

Teodoridis, V., J. Kovar-Eder, P. Marek, Z. Kvaček & P. Mazouch 2011. The integrated plant record vegetation analysis: internet platform and online application. *Acta Musei Nationalis Pragae, Series B – Historia Naturalis* 67(3–4):159–165.

Teodoridis, V., Z. Kvaček & T. Utescher 2021. The IPR-vegetation analysis as a tool for palaeoecological and palaeoclimatological reconstruction. In: *Methods in palaeoecology: Reconstructing Cenozoic terrestrial environments and ecological communities* (D.A. Croft, D.F. Su & S.W. Simpson, eds), pp. 151–171, Springer, Cham.

Thompson, N., U. Salzmann, D.K. Hutchinson, S.L. Strother, M.J. Pound, T. Utescher, J. Brugger, T. Hickler, E.P. Hocking & D.J. Lunt 2025. Global vegetation zonation and terrestrial climate of the warm Early Eocene. *Earth-Science Reviews* 261:105036.

Utescher, T. & V. Mosbrugger 2007. Eocene vegetation patterns reconstructed from plant diversity – A global perspective. *Palaeogeography, Palaeoclimatology, Palaeoecology* 247(3–4):243–271.

Utescher, T., A. Dreist, A.-J. Henrot, T. Hickler, Y.-S. Liu, V. Mosbrugger, F.T. Portmann & U. Salzmann 2017. Continental climate gradients in North America and Western Eurasia before and after the closure of the central American Seaway. *Earth and Planetary Science Letters* 472:120–130.

Utescher, T., B. Erdei, L. François, A.-J. Henrot, V. Mosbrugger & S. Popova 2021. Oligocene vegetation of Europe and western Asia – Diversity change and continental patterns reflected by plant functional types. *Geological Journal* 56(2):628–649.

Vasilieva, O.N. & A.P. Levina 2007. Organic-walled phytoplankton in the Upper Cretaceous and Paleogene sediments of the Kushmurun section of the Turgay trough (Kazakhstan). *Byulleten' Moskovskogo obshchestva ispytatelei pripody. Otdel geologicheskii* 82(2):40–55 (in Russian). [Васильева О.Н., Левина А.П. 2007. Органикостенный фитопланктон в верхнемеловых и палеогеновых отложениях разреза Кушмурун Тургайского прогиба (Казахстан) // Бюллетень МОИП. Отд. геол. Т. 82, № 2. С. 40–55].

Wang, J., Y.J. Wang, Z.C. Liu, J.Q. Li & P. Xi 1999. Cenozoic environmental evolution of the Qaidam Basin and its implications for the uplift of the Tibetan Plateau and the drying of central Asia. *Palaeogeography, Palaeoclimatology, Palaeoecology* 152(1–2):37–47.

Westerhold, T., N. Marwan, A.J. Drury, D. Liebrand, C. Agnini, E. Anagnostou, J.S.K. Barnet, S.M. Bohaty, D. De Vleeschouwer, ... & J.C. Zachos 2020. An astronomically dated record of Earth's climate and its predictability over the last 66 million years. *Science* 369(6509):1383–1387.

Willis, K.J. & J.C. McElwain 2002. *The evolution of plants*. Oxford University Press, Oxford, 378 pp.

Wing, S.L. & L.D. Boucher 1998. Ecological aspects of the Cretaceous flowering plant radiation. *Annual Review of Earth and Planetary Sciences* 26: 379–421.

Wolfe, J.A. 1979. Temperature parameters of humid to mesic forests of eastern Asia and relation to forests of other regions of the Northern Hemisphere and Australasia. *U.S. Geological Survey Professional Paper* 1106, 37 pp.

Wolfe, J.A. 1985. Distribution of major vegetational types during the Tertiary. In: *The carbon cycle and atmospheric CO_2: Natural variations Archean to present (Geophysical Monograph Series 32)* (E.T. Sundquist & W.S. Broecker, eds), pp. 357–375, American Geophysical Union,Washington, D.C.

Xie, Y.L., F.L. Wu, X.M. Fang, D.W. Zhang, &W.L. Zhang 2020. Early Eocene southern China dominated by desert: evidence from a palynological record of the Hengyang Basin, Hunan Province. *Global and Planetary Change* 195:103320.

Xie, Y.L., F.L. Wu & X.M. Fang 2022. A transient south subtropical forest ecosystem in central China driven by rapid global warming during the Paleocene–Eocene Thermal Maximum. *Gondwana Research* 101:192–202.

Yuan Q., Barbolini N., Rydin C., Gao D.-L., Wei H.-C., Fan Q.-S., Yang Y.-P., Liu X.-Y., Vajda V., Yang W.-L., Li S.-F.,

Zhang H., Wu Y., Liu J.-Q. 2020. Aridification signatures from fossil pollen indicate a drying climate in east-Central Tibet during the late Eocene. Climate of the Past 16(6): 2255–2273.

Zachos, J.C., M. Pagani, L. Sloan, E. Thomas & K. Billups 2001. Trends, rhythms, and aberrations in global climate 65 Ma to present. *Science* 292(5517):686–693.

Zachos, J.C., G.R. Dickens & R.E. Zeebe 2008. An early Cenozoic perspective on greenhouse warming and carbon-cycle dynamics. *Nature* 451(7176):279–283.

Zhang, J.Y., Y.J. Peng & J. Liu 2007. An important discontinuity of the Paleogene volcanic incidents in northeast China and their prospecting significance. *Jilin Geology* 26(2):1–7 (in Chinese with English abstract).

Zhang, R., D. Jiang, C. Zhang & Z. Zhang 2022. Distinct effects of Tibetan Plateau growth and global cooling on the eastern and central Asian climates during the Cenozoic. *Global and Planetary Change* 215:103854.

Zhang, Z., F. Flatøy, H. Wang, I. Bethke, M. Bentsen & Z. Guo 2012. Early Eocene Asian climate dominated by desert and steppe with limited monsoons. *Journal of Asian Earth Sciences* 44:24–35.